JOURNAL OF CATALYSIS 97, 156–168 (1986)

HCN Synthesis from CH_4 and NH_3 on Platinum[1]

D. HASENBERG AND L. D. SCHMIDT

Department of Chemical Engineering and Materials Science, University of Minnesota, Minneapolis, Minnesota 55455

Received May 6, 1985; revised July 23, 1985

The kinetics of HCN synthesis from CH_4 and NH_3 were studied for pressures between 0.05 and 5.0 Torr and temperatures between 500 and 1500 K on a clean polycrystalline Pt foil using a reaction chamber attached to an ultrahigh vacuum analysis chamber for contamination-free surface characterization. Rates are fit accurately by a modified Langmuir–Hinshelwood model that assumes surface carbon as both a reactant and a catalyst poison. Surfaces were cleaned in the ultrahigh vacuum chamber as determined by Auger electron spectroscopy. Postreaction Auger electron spectroscopy and temperature-programmed desorption analyses showed that the active surface contained less than a monolayer of carbon, while a surface deactivated in excess CH_4 contained multilayers of carbon. The rate and selectivity of HCN formation were slightly higher on Pt than on Rh, and the inhibition by carbon was less strong on Pt. Ethylene addition strongly poisoned the Pt surface by formation of carbon multilayers. Decomposition of CH_4 and C_2H_4 on Pt are also examined.

INTRODUCTION

Hydrogen cyanide, an important chemical intermediate in nylon production, is prepared by reaction of NH_3, CH_4, and O_2 over Pt–10% Rh gauzes. Yields up to 70% can be obtained industrially by reacting an approximately 1 : 1 : 1 mixture at 1400 K with a catalyst contact time of $\sim 10^{-3}$ sec. This high temperature requires that surface coverages of most species be very low, and the short contact time requires that all rate processes be very fast.

We have been studying the reactions in this system over polycrystalline Pt and Rh foils and wires in a reactor attached to an ultrahigh vacuum (UHV) system for surface analysis before and after reaction. In a previous paper (*1*), we reported kinetics and surface compositions in the reactions

$$NH_3 + CH_4 \rightarrow HCN + 3H_2 \quad (1)$$

and

$$2NH_3 \rightarrow N_2 + 3H_2 \quad (2)$$

on clean polycrystalline Rh. We showed that all rates over wide ranges of surface temperatures, gas compositions, and pressures could be fit semiquantitatively by modified Langmuir–Hinshelwood (LH) rate expressions

$$r_{HCN} = k_{HCN}\theta_c(1 - \theta_C)^n P_{NH_3} \quad (3)$$

$$= \frac{4.5 \times 10^{18} \exp(-1000/T) P_{CH_4} P_{NH_3}^5}{(1 + 0.0367 \exp(2500/T) P_{CH_4}/P_{NH_3}^5)^5} \quad (4)$$

and

$$r_{N_2} = k_{N_2}(1 - \theta_C)^n P_{NH_3} \quad (5)$$

$$= \frac{7.5 \times 10^{18} \exp(-2130/T) P_{NH_3}}{(1 + 0.0367 \exp(2500/T) P_{CH_4}/P_{NH_3}^5)^4} \quad (6)$$

where r is in molecules per square centimeter second and pressures are in Torr.

This mechanism implies that carbon (coverage θ_c) blocks n NH_3 adsorption sites. For Rh, we attained good agreement with all rate data assuming $n = 4$. We also showed that the carbon coverage measured by Auger electron spectroscopy (AES) cor-

[1] This work partially supported by NSF under Grant DMR 82126729.

0021-9517/86 $3.00

relates with this mechanism because $\theta_C < 1$ if the reaction was run with $P_{CH_4} < P_{NH_3}$ while $\theta_C \geq 1$ if $P_{CH_4} \geq P_{NH_3}$. However, for that system the carbon AES peak at ~270 eV overlaps Rh peaks so that it was possible to determine carbon coverages only qualitatively.

In this paper we report kinetics and surface coverages for the $NH_3 + CH_4$ reaction on polycrystalline Pt. Our objectives are to contrast rates on Pt and Rh and to determine accurately the coverages and characteristics of carbon on the active and inactive Pt catalyst.

EXPERIMENTAL

The experimental procedures for HCN synthesis on platinum were identical to those used for the study of rhodium (*1*). Platinum foils were cleaned by heating to 1500 K in 1×10^{-7} Torr of oxygen until only platinum and calcium peaks remained. This procedure typically required approximately 30 min. Calcium (if present) was removed by subsequent heating in 1×10^{-2} Torr of nitric oxide for 15 min at 1500 K followed by heating in vacuo at 1700 K. The foil was cycled through this process until only platinum peaks remained. The amount of calcium and the number of cycles required to remove it varied widely between different foil samples. An AES spectrum of a clean platinum surface is shown in Fig. 1.

The sample could be transferred from the UHV chamber to a steady-state flow reactor while remaining under vacuum. Magnetically coupled transfer rods were used to move the sample. Transfer and coupling to electrical feedthroughs typically required one minute or less to complete. The details of the transfer process are described elsewhere (*1*).

High purity gases were admitted into the flow reactor at the desired partial pressures through bakeable valves and lines with online cryogenic and adsorbent purification. The foil was heated resistively to the desired temperature. Rates generally attained

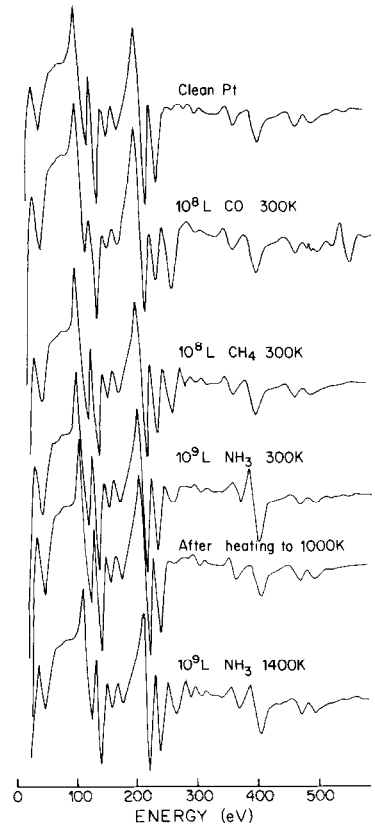

FIG. 1. AES spectra of a clean platinum foil and of the same foil after exposure to various gases at 10^8–10^9 L. Exposure to NH_3 produced less than 0.3 monolayers of carbon, and exposure to all other gases produced no measurable impurities.

steady-state values quickly, and no evidence of hysteresis was noted. Because the reaction is strongly endothermic (ΔH^0 of reaction 1 is +60 kcal/mole), multiple steady states should not be possible, and none were found. The rate of N_2 formation was found to attain unique steady-state values rapidly when P_{CH_4} was less than P_{NH_3}. Steady-state rates were more difficult to obtain in a large excess of CH_4 because of transients (the time to steady state was typically 1 to 5 min). It is believed that this transient behavior was due to carbon slowly building to its steady-state coverage on the platinum surface.

Most results were repeated on five foils with a reproducibility of ±20%. Rates are

based on the geometric area of the foil. The scanning electron microscope (SEM) revealed no evidence of pit formation or facets on Pt after reaction in contrast to that observed on Rh (*1*).

RESULTS

Ammonia Decomposition Kinetics

Ammonia decomposition on polycrystalline Pt was studied by Loffler and Schmidt (*2*). They reported the following LH rate expression found by fitting their data to a model for unimolecular decomposition,

$$r_{N_2} = \frac{4.9 \times 10^{18} \exp(-2130/T) P_{NH_3}}{1 + 4.35 \times 10^{-5} \exp(8400/T) P_{NH_3}} \quad (7)$$

where r_{N_2} is the rate of N_2 formation in molecules per square centimeter second and P_{NH_3} is in torricellis. The data for ammonia decomposition were readily reproduced in the present apparatus (now shown to be on a clean Pt surface). Measured rates were always within a factor of 2 of the above rate expression on at least 10 different platinum foils. The AES spectra following exposure to ammonia at 300 and 1400 K are shown in Fig. 1. These spectra show that after exposure to 1×10^9 L of ammonia at 300 K, the surface after pumpdown contained a monolayer of nitrogen (*3*) and that this nitrogen layer desorbs completely after flashing in vacuo to 1000 K.

The rate of ammonia decomposition on platinum is about one-half of the rate of ammonia decomposition on rhodium. The apparent activation energies are nearly identical on both metals. These findings also agree with recent comparisons between Pt and Rh by Papapolymerou and Schmidt (*4*). Since Rh foils facet during reaction, these results show that the rate of NH_3 decomposition is essentially identical on both metals.

HCN Synthesis Kinetics

Thermodynamic equilibrium in a 1 : 1 gas mixture favors N_2 formation over HCN formation at all temperatures below 1600 K. The rate of NH_3 decomposition exceeds 10^{18} molecules/cm^2 sec at 1500 K in 1 Torr ammonia. This reaction rate is high enough to make the reaction of NH_3 with any other species on platinum at 1500 K very unlikely unless ammonia decomposition can be inhibited. The probability of an incident ammonia molecule decomposing to N_2 and H_2 is greater than 0.001 on platinum a 1500 K and the coverage of ammonia at this tem-

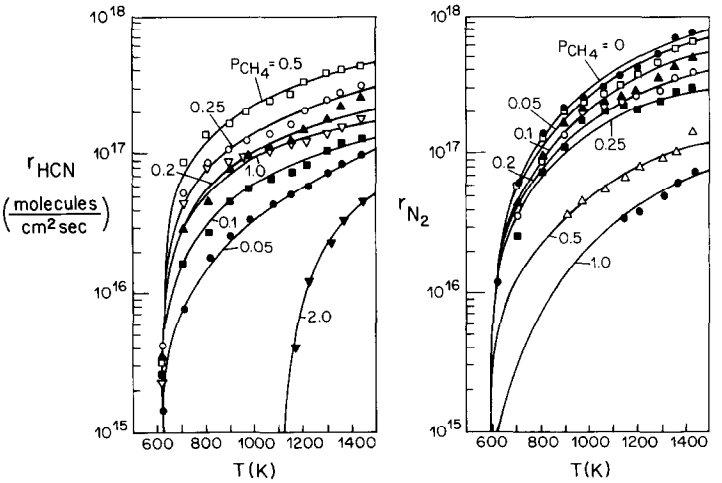

FIG. 2. Rates of HCN and N_2 formation versus platinum foil temperature for P_{NH_3} = 0.5 Torr at the methane pressures indicated. The solid curves connect the data points of a fixed methane pressure.

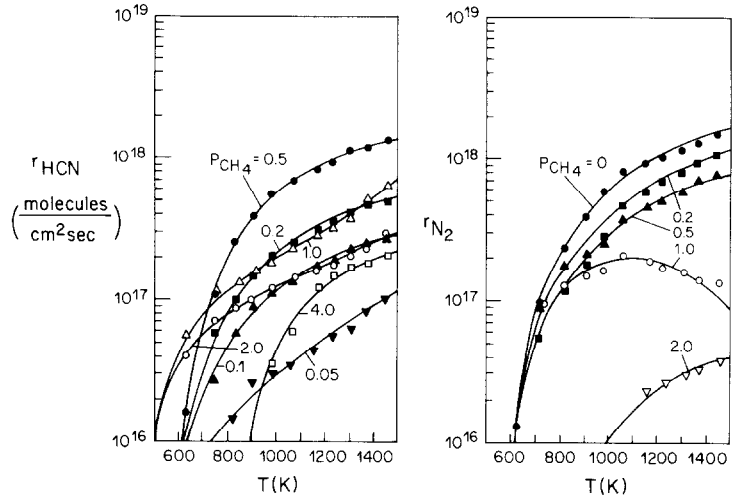

FIG. 3. Rates of HCN and N_2 formation versus platinum foil temperature for P_{NH_3} = 1.0 Torr at the methane pressures indicated.

perature is estimated to be less than 10^{-5} monolayers assuming a heat of adsorption of 20 kcal/mole (*5*). The prospect of producing HCN from methane and ammonia on platinum thus seems poor when confronted with both thermodynamic equilibria and the rate of ammonia decomposition.

Figures 2 and 3 show the reaction rates vs temperature for HCN and N_2 formation on Pt at P_{NH_3} = 0.500 and 1.00 Torr, respectively. Solid lines are smooth curves drawn to connect the data points. It is seen that r_{HCN} shows no maximum versus temperature and that r_{N_2} has no maximum except when a stoichiometric excess of methane is present. It is seen that the rate of HCN production is proportional to P_{CH_4} for low methane pressures and that r_{HCN} is inhibited strongly by methane in a stoichiometric excess of methane.

Figure 4 shows r_{HCN} and r_{N_2} versus P_{CH_4} at 1450 K. It is seen that r_{HCN} is first order in methane at low P_{CH_4} and is inhibited by methane at high P_{CH_4} approximately as $P_{CH_4}^{-3}$. Similarly, r_{N_2} is zero order in P_{CH_4} at low P_{CH_4} and becomes inhibited as $P_{CH_4}^{-3}$ at high methane pressures.

It can also be seen that the reaction rate

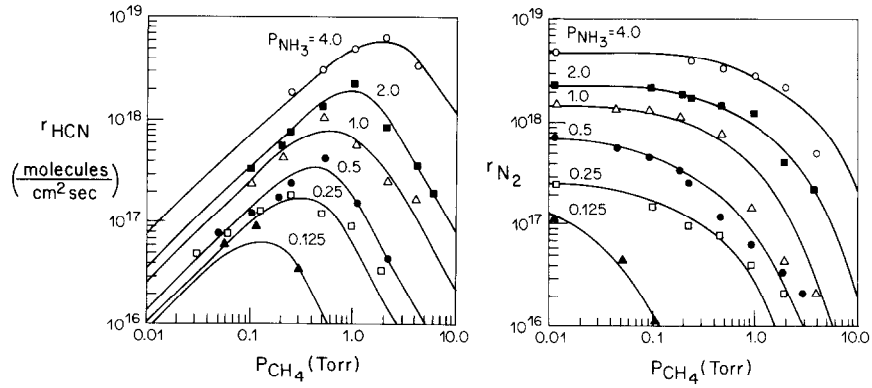

FIG. 4. Rates of HCN and N_2 formation on platinum at 1450 K versus P_{CH_4} at the ammonia pressures indicated. HCN production increases with P_{CH_4} and goes through a maximum rate near a 1 : 1 reactant ratio. The rate falls quickly in excess methane. Nitrogen formation is independent of P_{CH_4} at low P_{CH_4} and is inhibited strongly in excess methane.

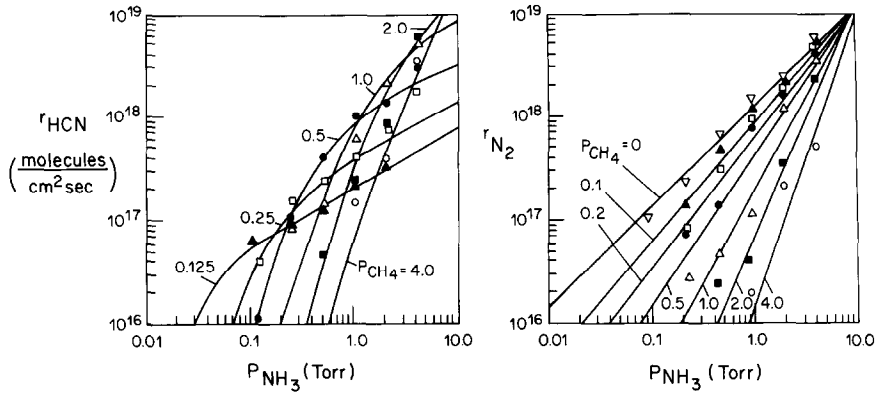

FIG. 5. Rates of HCN and N_2 formation on platinum at 1450 K versus P_{NH_3} at methane pressures indicated. r_{HCN} varies from third order to half order in P_{NH_3} and r_{N_2} varies from first order to third order in P_{NH_3}.

falls with increasing P_{CH_4} when the surface is at 1450 K. Therefore, it is argued that homogeneous reactions are not significant in the kinetics of HCN synthesis. If free radicals desorbing from the surface induced any gas phase chemistry then, because the surface is still hot, there should be no reason for rates to be inhibited by a slight excess of methane in the reactant mixture.

Figure 5 shows the ammonia dependences of r_{HCN} and r_{N_2} at 1450 K. The rate of HCN production is $\sim\frac{1}{2}$ order in ammonia in excess P_{NH_3} and increases to nearly third order in excess methane; r_{N_2} is first order in ammonia in the absence of methane and increases to approximately third order in excess methane.

Surface Characterization

Figure 6 shows AES spectra of a clean platinum surface and after heating in 10^8 L of methane at 1450 K. Heating in pure methane produces a graphitic peak so large that the major platinum peaks are almost totally obscured. Heating a clean platinum surface in a 2 : 1 methane to ammonia mixture (Fig. 7) produces a multilayer carbon coverage, but the thickness of this layer, estimated at ~15 Å (*6*), does not obscure the underlying platinum. There is also some nitrogen present on this surface. Heating to 1450 K in a 10^9-L exposure to 1 : 1 meth-

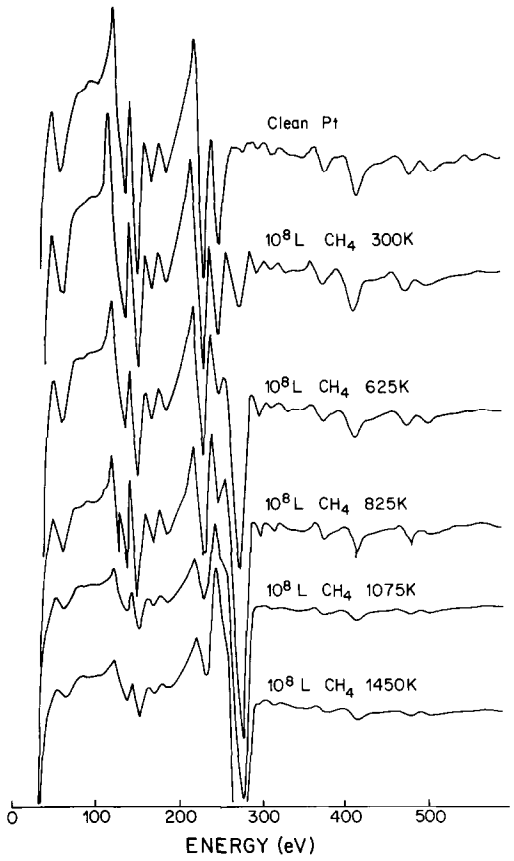

FIG. 6. Auger spectra of a clean Pt foil and of the same foil after exposure to 10^8 L methane at foil temperatures indicated. The carbon line shape following a 10^8-L exposure at 300 K is indicative of carbidic carbon.

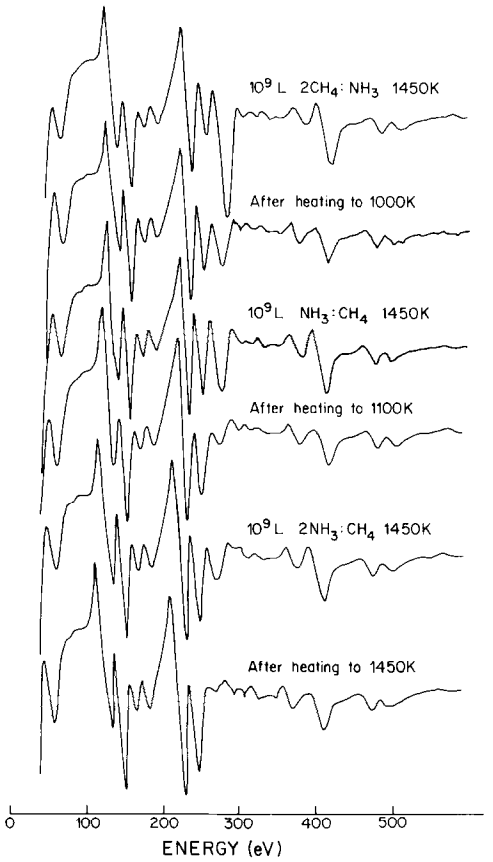

FIG. 7. AES spectra of platinum foil after heating to 1450 K in mixtures of methane and ammonia as indicated. It is seen that the carbon peak that is formed can be quantitatively measured. Less than a monolayer of carbon is present on the active ($2NH_3$: $1CH_4$) surface.

ane and ammonia produces slightly more than a monolayer of carbon and less than a monolayer of nitrogen. This surface retains a fraction of a monolayer of carbon after flashing to 1000 K in vacuo. The 270-eV carbon peak does not overlap with any platinum peaks and therefore the carbon signal can be measured more quantitatively than on rhodium where peaks overlap.

It is possible to determine the nature of adsorbed carbon from the line shape of the carbon 270-eV peak (*7*). The carbon signal from the adsorption of 10^8 L of methane at 300 K (Fig. 1) is indicative of carbidic carbon which is bonded to the metal surface only and not to neighboring carbon atoms. The second type of carbon peak is seen when 10^8 L of methane is exposed to platinum at 1450 K (Fig. 6). This carbon Auger line shape is characteristic of a graphitic carbon that is bonded to neighboring carbon atoms. Van Langeveld *et al.* (*8*) have shown that the carbidic carbon form is much more reactive than the graphitic carbon in forming methane in the CO–H_2 reaction on platinum.

Figure 8 shows temperature-programmed desorption (TPD) spectra from a platinum foil after various exposures to methane and ammonia. TPD spectra following exposures of mixtures of gases to platinum at 1450 K were obtained by letting the surface cool to room temperature and then pumping out the gases to $\sim 10^{-8}$ Torr prior to flashing the surface. A 10^9-L exposure to ammonia resulted in a large N_2 peak. This result agrees with AES spectra of Fig. 1 and also with the data of Mummey and Schmidt (*3*) who showed that this peak is a monolayer of nitrogen as determined by calibration against a saturation CO exposure. Our results show that nitrogen coverages are reduced 90% by the presence of methane. Therefore, nitrogen on the surface desorbs preferentially as HCN and not as N_2 when adsorbed CH_4 is present on the surface.

The results also show that there is approximately a quarter monolayer of hydrogen present after exposure to 10^9 L of ammonia and that the presence of methane reduces the coverage of hydrogen. There is no desorbing H_2 present at all following a 10^8-L exposure to methane at 300–1450 K. Hydrogen adsorption on platinum was studied by McCabe and Schmidt (*9, 10*) who found that H_2 desorbs between 200 and 400 K. No new states of adsorbed H_2 were found after exposure to methane or ammonia in any of the experiments reported here.

HCN desorbed at ~440 K in the TPD experiments, but coverages were usually much less than a CO monolayer. The nitrogen observed in the AES spectra of Fig. 7 desorbs mostly as HCN rather than as N_2 or NH_3. Hydrogen cyanide adsorption on plat-

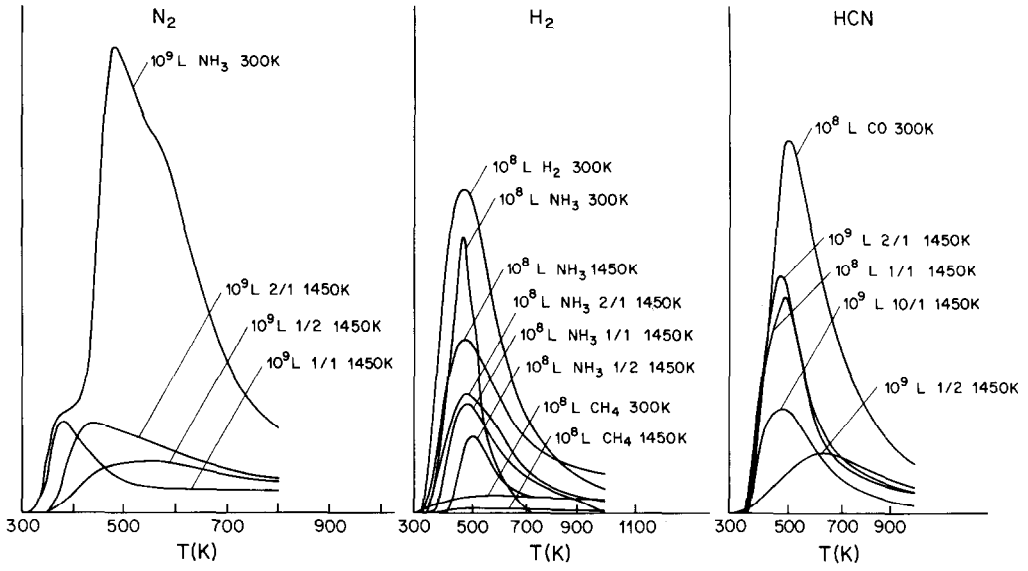

FIG. 8. TPD spectra of N_2, H_2, and HCN following cooling and pumpdown after simulated reaction conditions as indicated. Heating rates were roughly 50 K/sec. N_2 formation is inhibited by the presence of methane.

inum has been studied by Bridge and Lambert (*11*, *12*). They found that HCN adsorbed on platinum at 300 K at low exposures desorbs as H_2, HCN, and C_2N_2, with H_2 and HCN desorbing at ~400 K and cyanogen desorbing in two states at 873 and 930 K.

Figure 6 shows the Auger spectra of a clean platinum surface and of the same surface after heating in methane at various temperatures. It is seen that a 10^8-L exposure of methane at 300 K produces ~$\frac{3}{4}$ monolayer of carbon on the surface (calibrated against the C_{270} signal from a CO monolayer). This carbon desorbs completely by heating in vacuo to the relatively low temperature of 500 K.

When platinum is heated in the presence of pure methane, a non-desorbing carbon residue is formed which is stable to the melting point of platinum. The surface of the platinum foil was cleaned between each spectrum shown in Fig. 6 so that the surface was clean initially before each successive exposure to methane. It is seen that the rate of carbon deposition is a strong function of the foil temperature.

Effect of Ethylene Addition

The addition of small amounts of ethylene to ammonia greatly inhibits the rate of ammonia decomposition. In Fig. 9, the rate of N_2 formation from 1 Torr ammonia and the rate of HCN formation from 1 Torr of

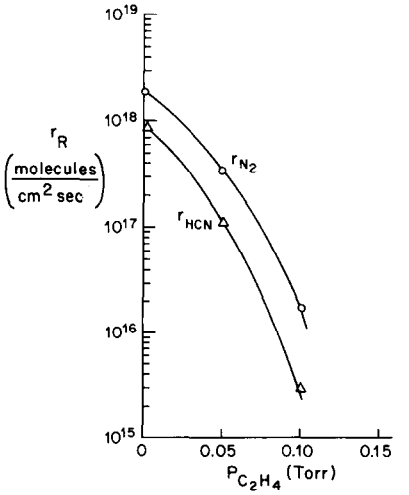

FIG. 9. Plots of r_{N_2} ad r_{HCN} versus $P_{C_2H_4}$ at 1450 K. The addition of 10% ethylene to the reactant stream effectively poisons the platinum surface so that no reactions occur.

both methane and ammonia at 1450 K vs $P_{C_2H_4}$ are plotted. It is seen that the addition of 5% ethylene is enough to inhibit the rates of HCN and N_2 production by an order of magnitude. Adding 10% ethylene totally quenches both reactions at 1450 K.

Surface graphite layers formed by heating in ethylene or methane at high temperatures are difficult to remove by low pressure O_2 treatment of the foil. Heating to 1500 K in 10^{-7} Torr of oxygen for 2 hr did not measurably affect the amount of carbon on the surface, although heating to 1500 K in 0.1 Torr of oxygen removes this carbon layer in 1–5 min. The ability of oxygen to continuously clean the surface is probably essential to the success of the commercial Andrussow process. Unless the methane feed in the Degussa process is totally free of carbon-forming species such as ethylene, propylene, butadiene, benzene, etc., the catalyst surface should be very rapidly deactivated by buildup of graphite.

Methane and Ethylene Decomposition

The rate of carbon deposition on platinum can be determined accurately by monitoring the total pressure in the reactor operated in the batch mode by charging to a specified initial pressure of CH_4 or C_2H_4 and monitoring total and partial pressures versus time (*13*). Adsorption of 10^{-3} Torr on 1 cm^2 of surface corresponds to one monolayer in a 0.5-liter chamber. The rate of methane decomposition

$$CH_4 \rightarrow C + 2H_2 \qquad (8)$$

is therefore easily determined and the coverage of carbon can be estimated.

Figure 10 shows the pressure rise when 0.5 Torr of CH_4 is exposed to platinum at 1400 K. Initially the decomposition rate was very high ($>10^{18}$ molecules/cm^2 sec). After several seconds, the rate slowed to $\sim 5 \times 10^{15}$ molecules/cm^2 sec and then steadily decreased to a low value. Other investigators (*14*) have shown that after this incubation period (approximately 30 min), a rapid filamentous carbon growth regime is entered. The rate of ethylene decomposition is also shown in Fig. 10 and it is seen to be $\sim\frac{1}{3}$ of the integral rate of methane decomposition. Ethylene probably poisons the surface with graphite formation faster than methane can build up a graphite layer. In both cases, the reaction consumes less than 10% of the reactants even after 30 min at 1400 K. The results show that twice as much CH_4 decomposes on Pt after 20 min than C_2H_4. Since CH_4 should deposit one-half as much carbon as does C_2H_4, it is inferred that the same coverage of carbon is necessary in each case to deactivate the surface.

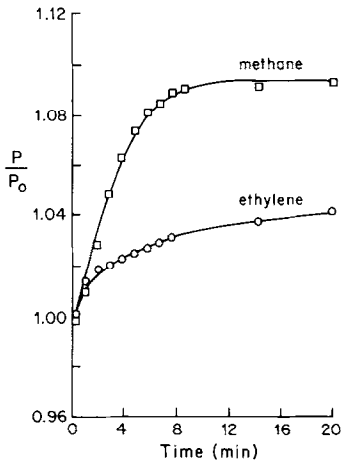

FIG. 10. Integral rate of both methane and ethylene decomposition on Pt at 1450 K.

Deuterium Exchange Reactions

In an attempt to determine the surface activity of methane, the deuteration rate of CH_4 on Pt was examined qualitatively. Kemball (*15, 16*) *et al.* have reported deuteration exchange rates of CH_4 on Pt, Ni, Rh, and Pd evaporated metal films, although they did not calibrate rates because areas of their films were not known.

The methane–D_2 exchange rate is shown in Fig. 11. The mass 16 (CH_4) and 17 (CH_3D) signals were measured and the data are plotted as (mass 16)/(mass 16 + mass 17) vs time. At 1450 K, the rate of exchange is zero. This is undoubtedly because the

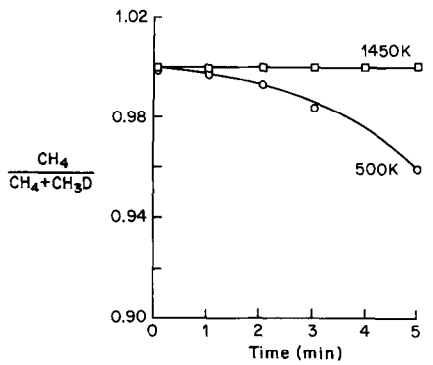

FIG. 11. The rate of deuterium–hydrogen exchange on Pt at both 1450 and 500 K. The data are plotted as the ratio of the height of the mass 16 (CH_4) peak and the sum of the CH_4 and mass 17 (CH_3D) peaks versus time. It is seen that at 1450 K, the rate of reaction is too small to measure.

surface is poisoned by a graphite layer. At 500 K, the rate is exceedingly small (less than 1×10^{14} molecules/cm^2 sec) but measurable. The rate of deuterium–hydrogen exchange in ethylene is extremely difficult to measure because of the complications arising from the hydrogenation reaction. This is a much studied reaction (*17*) which proceeds to completion in a few minutes on Pt at room temperature. The rate of this reaction is greater than 10^{18} molecules/cm^2 sec at 300 K. During HCN synthesis, when the presence of adsorbed NH_3 helps to preserve a clean Pt surface, the exchange rate of methane–D_2 is probably much higher than the rates measured here.

DISCUSSION

Kinetics

The rate of HCN synthesis on platinum was modeled in the same manner as on rhodium. That is, the data were fit to expressions of the form

$$r_{HCN} = \frac{k_{HCN} P_{CH_4} P_{NH_3}^{.5}}{(1 + K P_{CH_4}/P_{NH_3}^{.5})^{(n+1)}} \quad (9)$$

and

$$r_{N_2} = \frac{k_{N_2} P_{NH_3}}{(1 + K P_{CH_4}/P_{NH_3}^{.5})^{n}} \quad (10)$$

where $K = k_{a_{CH_4}}/k_{a_{NH_3}}$ and n is the number of sites that methane blocks.

The rate expressions found by fitting the data to the model are

$$r_{HCN} = \frac{7.8 \times 10^{18} \exp(-1950/T) P_{CH_4} P_{NH_3}^{.5}}{(1 + 0.044 \exp(2390/T) P_{CH_4}/P_{NH_3}^{.5})^4} \quad (11)$$

and

$$r_{N_2} = \frac{4.9 \times 10^{18} \exp(-2130/T) P_{NH_3}}{(1 + 0.044 \exp(2390/T) P_{CH_4}/P_{NH_3}^{.5})^3}. \quad (12)$$

Figures 12 and 13 show plots of the fits at 1450 K. All data are seen to be within a factor of 3 of the model. It is seen that n (the number of sites that each carbon atom blocks) is 3 in the above rate expressions.

The activation energy for HCN synthesis on platinum was found by the fit to the data between 1100 and 1450 K. The activation energy for HCN synthesis was found to be 4340 cal/mole (whereas on Rh the corresponding value was 3500 cal/mole). The activation energy for ammonia decomposition was found to be 4520 cal/mole on Pt and 4580 cal/mole on Rh. These values show that NH_3 decomposition energetics are almost identical for both metals. It is very likely that the mechanism for reaction is identical on both surfaces.

It is seen that the model correctly predicts the variable order dependences of both methane and ammonia. The methane dependence on r_{HCN} varies from first order in methane at low P_{CH_4} to negative third order at high P_{CH_4} (Fig. 12). Similarly, the ammonia dependence on r_{HCN} varies from half order at low P_{NH_3} to third order at high P_{NH_3} (Fig. 13). In the absence of methane, the model reduces to the rate expression for ammonia decomposition.

Suárez and Loffler (*18*) have reported the rate of HCN synthesis on Pt wires at 1 atm total pressure. Koberstein (*19*) has reported results from the operation of a bench scale Degussa reactor using a Pt catalyst. Our present data, when used to model the

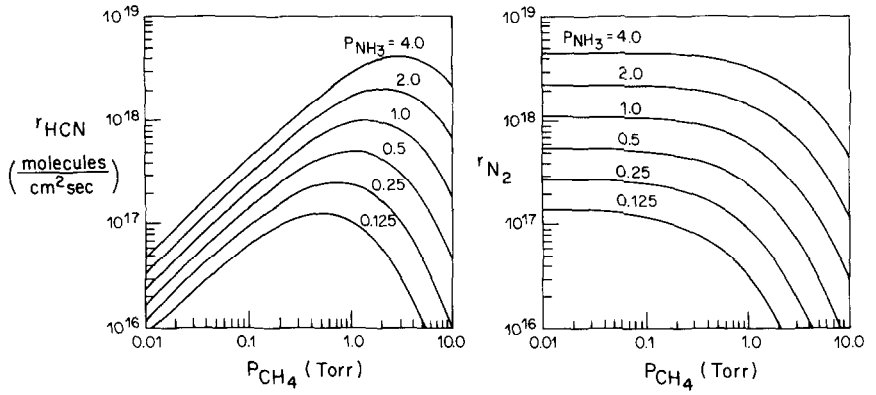

FIG. 12. Plots of r_{HCN} and r_{N_2} versus P_{CH_4} at 1450 K using the Langmuir–Hinshelwood model of Eqs. (11) and (12). The model is seen to be within a factor of 3 of the data points in Fig. 4.

atmospheric pressure process, agrees within 10% to the data taken at 1 atm, for temperatures between 1100 and 1500 K.

Surface Carbon

In Figure 14, The C_{270}/Pt_{238} ratio following a 10^8-L exposure to methane is plotted vs foil temperature for data from Fig. 6. The resulting curve is non-linear, and the upward concave behavior is probably due more to the Pt_{238} peak being attenuated than to the growth of the C_{270} peak. The thickness of the resulting carbon layers can be estimated by the method of Powell (*6*) as ~15 Å after heating to 1450 K in 10^8 L of methane, but the uncertainty in his calculation is 50% because of the large attenuation of the platinum peaks. This result shows that methane adsorption is both activated and irreversible at high temperatures.

Comparison of the TPD and AES data gives information on the nature of the active surface during HCN synthesis. The active platinum surface is covered with slightly less than a monolayer of carbon. This carbon layer inhibits N_2 formation as seen in the TPD spectra. Increasing methane concentrations produce multilayer carbon coverages which inhibit steady-state rates of both reactions. Auger spectra taken

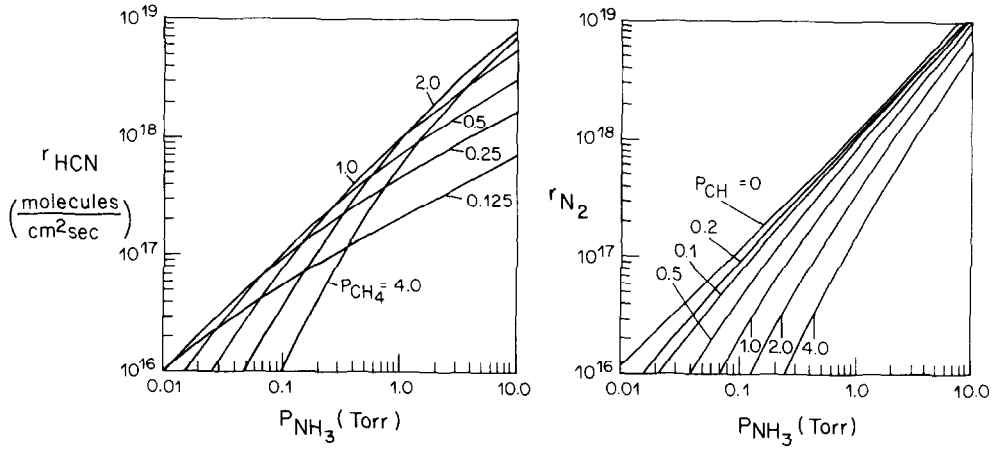

FIG. 13. Plots of r_{HCN} and r_{N_2} versus P_{NH_3} of the LH model of Eqs. (11) and (12) at 1450 K. The model agrees well with the data of Fig. 5.

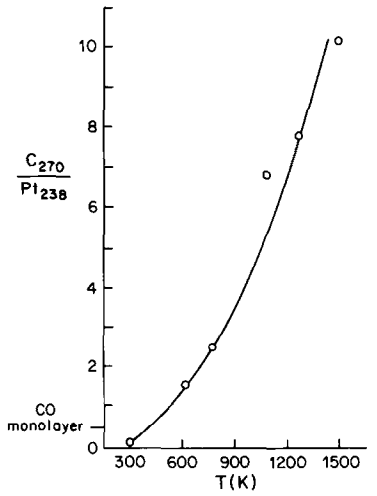

FIG. 14. Plot of the C_{270}/Pt_{238} Auger peak ratio following 10^8-L exposures to methane versus Pt foil temperature.

after the TPD spectra show that non-desorbing carbon is present on the low activity platinum surface. The thickness of this non-desorbing carbon layer increases with increasing P_{CH_4} at fixed P_{NH_3}. The absence of any desorbing methane or ammonia indicates that the reactive intermediate species are most probably atomic nitrogen and carbon. Because submonolayer amounts of carbon can be measured accurately, we estimate from the AES spectra of Fig. 7 that there is $\sim\frac{3}{4}$ monolayer of carbon present following HCN synthesis in equimolar methane : ammonia, and $\sim\frac{1}{4}$ monolayer carbon after $2NH_3:1CH_4$ HCN synthesis. There are ~2.5 monolayers of carbon following a 10^8-L exposure to $1NH_3:2CH_4$ at 1450 K.

Even in the case of excess methane, there is only a monolayer of non-desorbing carbon on the surface. After exposure to reactant mixtures containing an excess of ammonia, the surface has less than a monolayer of carbon after flashing in vacuo. Thus, HCN synthesis is possible because adsorbed NH_3 is able to prevent the large carbon accumulations at elevated temperatures shown in Fig. 14.

The theoretical values of the surface carbon coverage during reaction can be predicted by the following equation which is a result of the model for the kinetics (*1*),

$$\theta_C = \frac{KP_{CH_4}/P_{NH_3}^{.5}}{1 + KP_{CH_4}/P_{NH_3}^{.5}}. \qquad (13)$$

In Figure 15, the C_{270}/Pt_{238} peak ratio following heating in 10^9 L methane–ammonia mixtures is plotted against mole fraction (X) of methane. The solid curve is the value for θ_C predicted by Eq. (13). One monolayer of carbon is taken to be twice the amount of carbon present after a saturation exposure to CO at 300 K. It can be seen that the model successfully predicts carbon coverages in the ammonia excess regime. The theoretical values deviate from the experimental values in the methane excess regime becaue the model is strictly a monolayer model and it will never predict $\theta_C > 1$.

Comparison with Rhodium

Figure 16 shows r_{HCN} versus P_{CH_4} at 1450 K on both platinum and rhodium. It is seen that the two rates have similar magnitudes

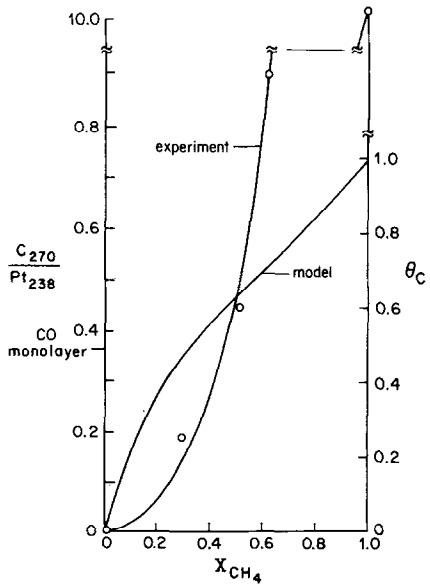

FIG. 15. Plot of the C/Pt Auger peak ratios versus mole fraction methane after heating a Pt foil in HCN synthesis conditions to 1450 K. The data are compared with the theoretical curve of Eq. (13) for the amount of carbon on the surface during reaction.

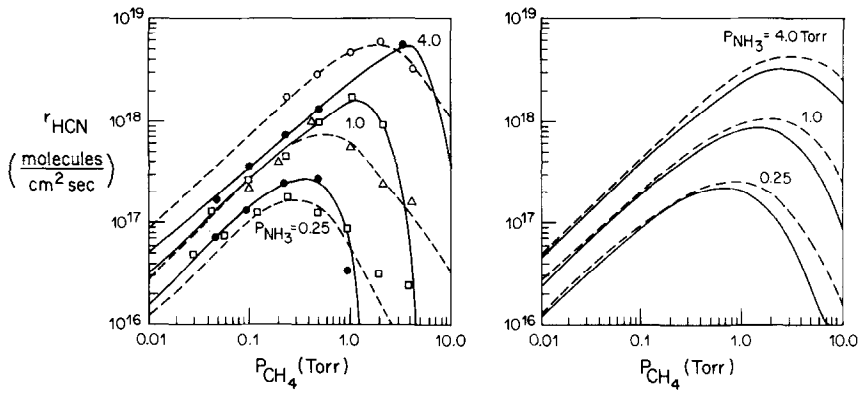

FIG. 16. The rates of HCN formation versus P_{CH_4} at 1450 K for both platinum (dashed lines) and rhodium (solid lines) are presented. It is seen that the two rates are nearly indistinguishable with the maximum rate on platinum being slightly greater than on rhodium. The data are presented in the left panel and the corresponding fits to the data using the Langmuir–Hinshelwood expressions of Eqs. (4) and (11) are presented in the right panel.

and pressure dependences with the maximum rate on platinum being slightly higher than on rhodium. Ammonia decomposition on rhodium is slightly faster than on platinum, but HCN synthesis is slightly faster on platinum. The activities of the two metals are within a factor of 2 at all temperatures in this pressure range. This is not surprising considering that the reaction takes place at 1450 K where surface adsorbate lifetimes are exceedingly short. Any incident molecule that does not immediately desorb must decompose and therefore transform into a product species. Surface morphology may account for the factor of 2 difference in rates between ammonia decomposition on Pt and Rh since faceting produces a rhodium surface area increase by a factor of ~2 whereas platinum does not facet significantly during these reactions.

The major difference between the two metals is the number of sites that methane blocks. On platinum, n was determined to be 3, whereas on rhodium, n was 4 (a better fit for Rh would in fact be obtained with $n >$ 4). This difference in CH_4 inhibition allows for a greater yield of HCN on platinum by using a reactant mixture richer in methane. These results therefore predict a better selectivity to HCN on platinum than on rhodium.

Comparison of TPD and AES spectra of the two metals shows that carbon forms more readily on Rh and more HCN desorbs (ratio of 3 : 1) from platinum following cooling and pumpdown after a 10^9-L exposure to a 1 : 1 mixture of methane and ammonia at a surface temperature of 1450 K. Nitrogen on Rh desorbs mainly as N_2 whereas HCN is the main nitrogen-containing desorption product on platinum. Rhodium also produces an AES carbon spectrum characteristic of graphite in methane–ammonia mixtures whereas on platinum the carbon spectrum is characteristic of carbide or a hydrocarbon layer. These results are all consistent with the fact that platinum is a better catalyst for HCN synthesis.

In determining which catalyst would be best suited for an actual HCN converter, both selectivity and activity need to be considered. We find that the activity on both metals is nearly identical and the selectivity to HCN then becomes the deciding issue. Because platinum has a better activity in the near stoichiometric reactant regime, it should give a better selectivity to HCN.

Therefore, platinum appears to be the catalyst of choice for HCN synthesis. Modeling studies on Pt and Rh using these kinetics will be reported in a later paper.

SUMMARY

The kinetics of the HCN synthesis reaction and the accompanying ammonia decomposition reaction were determined experimentally and could be fit quantitatively to a modified Langmuir–Hinshelwood rate expression. The same form of rate expression developed for HCN synthesis on rhodium fits the data for platinum with the only difference between Pt and Rh being that excess methane inhibits reaction rates on rhodium more than on platinum.

The mechanism of reaction that is most reasonable is also very simple. Incident reactant molecules that do not immediately desorb must instead decompose rapidly on the hot platinum surface. Simple molecules such as N_2 and H_2 are formed and rapidly desorb. A carbon layer formed from methane decomposition inhibits the rate of ammonia adsorption. This same carbon layer which poisons the surface by inhibiting ammonia decomposition reacts with surface nitrogen to form HCN. Thus, surface carbon both promotes HCN formation and inhibits N_2 formation. By regulating the coverage of this carbon layer by either adjusting the reactant mixture or including oxidizing reactants or by adding surface promoters, the conditions for HCN synthesis may be optimized. These procedures will be described in a later paper.

REFERENCES

1. Hasenberg, D., and Schmidt, L. D., *J. Catal.* **91,** 116 (1985).
2. Loffler, D. G., and Schmidt, L. D., *J. Catal.* **41,** 440 (1976).
3. Mummey, M. J., and Schmidt, L. D., *Surf. Sci.* **91,** 301 (1980).
4. Papapolymerou, G., and Schmidt, L. D., *Langmuir* **1,** 488 (1985).
5. Gland, J. L., *Surf. Sci.* **71,** 327 (1978).
6. Powell, C. J., *Surf. Sci.* **44,** 29 (1974).
7. Houston, J. E., Peebles, D. E., and Goodman, D. W., *J. Vac. Sci. Technol.* **A1,** 995 (1983).
8. Van Langeveld, A. D., Van Delft, F., and Ponec, V., *Surf. Sci.* **135,** 93 (1983).
9. McCabe, R. W., and Schmidt, L. D., *Surf. Sci.* **60,** 85 (1976).
10. McCabe, R. W., and Schmidt, L. D., *Surf. Sci.* **65,** 189 (1977).
11. Bridge, M. E., Marrow, R. A., and Lambert, R. M., *Surf. Sci.* **57,** 415 (1976).
12. Bridge, M. E., and Lambert, R. M., *J. Catal.* **46,** 143 (1977).
13. Suárez, M. P., Cechini, J. O., and Loffler, D. G., *J. Catal.* **89,** 527 (1984).
14. LaCava, A. I., Bernardo, C. A., and Trimm, D. L., *Carbon* **20,** 219 (1982).
15. Kemball, C., *Proc. R. Soc. A* **207,** 539 (1951).
16. Kemball, C., *Proc. R. Soc. A* **213,** 359 (1953).
17. Satterfield, C. N., "Heterogeneous Catalysis in Practice," p. 267. McGraw–Hill, New York, 1980.
18. Suárez, M. P., and Loffler, D. G., submitted for publication.
19. Koberstein, E., *Ind. Eng. Chem. Process Des. Dev.* **12,** 444 (1973).